

# Production of $\Lambda\Lambda$ and $\overline{\Lambda n}$ in central Pb+Pb collisions at $\sqrt{s_{NN}}=2.76$ TeV within a covariant coalescence model

Kai-Jia Sun<sup>1</sup> and Lie-Wen Chen<sup>\*1,2</sup>

<sup>1</sup>*Department of Physics and Astronomy and Shanghai Key Laboratory for Particle Physics and Cosmology, Shanghai Jiao Tong University, Shanghai 200240, China*

<sup>2</sup>*Center of Theoretical Nuclear Physics, National Laboratory of Heavy Ion Accelerator, Lanzhou 730000, China*  
(Dated: September 9, 2018)

We study the production of  $\Lambda\Lambda$  and  $\overline{\Lambda n}$  exotic states in central Pb+Pb collisions at  $\sqrt{s_{NN}} = 2.76$  TeV at LHC via both hadron and quark coalescence within a covariant coalescence model with a blast-wave-like parametrization for the phase-space configurations of constituent particles at freezeout. In the hadron coalescence, the two states are considered as molecular states while they are considered as six-quark states in the quark coalescence. For  $\overline{\Lambda n}$ , we find that the yields of both molecular and six-quark states are much larger than the experimental upper-limits. For  $\Lambda\Lambda$ , while the molecule-state yield is much larger than the experimental upper-limits, the six-quark-state yield could be lower than the upper-limits. The higher molecule-state yields are mainly due to the large contribution of short-lived strong resonance decays into (anti-)nucleons and (anti-) $\Lambda$  which can significantly enhance the molecule-state yields of  $\Lambda\Lambda$  and  $\overline{\Lambda n}$  via hadron coalescence. Our results suggest that the current experimental measurement at LHC cannot exclude the existence of the  $\Lambda\Lambda$  as an exotic six-quark state, and if  $\Lambda\Lambda$  is a six-quark state, it is then on the brink of being discovered.

PACS numbers: 25.75.-q, 25.75.Dw

## I. INTRODUCTION

The conventional hadron spectrum can be well understood in quark model in which mesons are considered to consist of a quark and an anti-quark while (anti)baryons consist of three (anti)quarks. However, the fundamental theory of strong interaction, Quantum Chromodynamics (QCD) does not forbid the existence of exotic states with more than three valence quarks such as tetraquarks, pentaquarks, hexquarks, and so on. Jaffe [1] first predicted the existence of H-dibaryon, a hypothetical bound state consisting of  $uuddss$  with spin-parity  $J^\pi = 0^+$ , using a bag model approach. Lattice QCD (LQCD) calculations [2, 3] also suggest the bound H-dibaryon with strangeness  $S = -2$  and spin-parity  $J^\pi = 0^+$  may exist, although this needs to be confirmed by the physical point simulations [4]. A relevant and interesting question is about the possible existence of other exotic dibaryon states including nucleon-hyperon bound states like  $\Lambda n$  with  $S = -1$  and  $J^\pi = 1^+$  [5]. These studies would be extremely useful for understanding the largely uncertain nucleon-hyperon and hyperon-hyperon interactions.

To understand the  $\Lambda$ - $\Lambda$  interaction, the STAR collaboration [6] at Relativistic Heavy-Ion Collider (RHIC) recently measured the  $\Lambda$ - $\Lambda$  correlation function for centrality 0 – 80% Au+Au collisions at  $\sqrt{s_{NN}} = 200$  GeV. In Ref. [6], a positive scattering length  $a_0 > 0$  (decreasing phase shift) is obtained by analyzing the data using Lednicky-Lyuboshits (LL) model formula. However, an opposite sign of  $a_0$  is favored [7] by using Koonin-

Pratt (KP) formula. These two apparently contradictory conclusions can be understood [8] in the LL model formula with different values of  $\Lambda$ - $\Lambda$  pair purity probability  $\lambda$  which is still largely uncertain. Therefore, more experimental measurements are needed to further constrain the details of the  $\Lambda$ - $\Lambda$  interaction so as to determine if the bound  $\Lambda\Lambda$  state can exist or not.

Very recently, the ALICE collaboration [9] at Large Hadron Collider (LHC) searched for weakly decaying  $\Lambda\Lambda$  and  $\overline{\Lambda n}$  exotic bound states in central Pb+Pb collisions at  $\sqrt{s_{NN}} = 2.76$  TeV, and no bound states of  $\Lambda\Lambda$  and  $\overline{\Lambda n}$  are measured in the decay modes  $\overline{\Lambda n} \rightarrow \bar{d}\pi^+$  and H-dibaryon  $\rightarrow \Lambda p\pi^-$ . The obtained upper-limits of the yields ( $dN/dy$  at mid-rapidity) are found to be, in a large range of decay branching ratio (BR), much lower than the predictions of various models, including the equilibrium thermal model [10], the non-equilibrium thermal model [11, 12], a hybrid UrQMD calculation [5], and the coalescence model in which they are assumed to be molecular states (with hadron coalescence) or six-quark states (with quark coalescence) [13, 14]. The comparison between the experimental measurement and these existing model predictions seems to exclude the existence of the  $\Lambda\Lambda$  and  $\overline{\Lambda n}$  exotic bound states. However, we note that the coalescence model predictions of H-dibaryon in Refs. [13, 14]) are made only for central Au+Au (Pb+Pb) collisions at  $\sqrt{s_{NN}} = 200$  GeV (5.5 TeV) at RHIC (LHC) based on a significantly simplified approximate analytic formula of the coalescence model [13, 14]. Therefore, it is interesting to explore the production of  $\Lambda\Lambda$  and  $\overline{\Lambda n}$  in central Pb+Pb collisions at  $\sqrt{s_{NN}} = 2.76$  TeV in a more realistic coalescence model, and see if the experimental limits can or not exclude the existence of  $\Lambda\Lambda$  and  $\overline{\Lambda n}$  as molecular states or six-quark states. This is the main

\*Corresponding author: lwchen@sjtu.edu.cn

motivation of the present work.

In this paper, we carefully calculate the yields of the  $\Lambda\Lambda$  and  $\overline{\Lambda n}$  exotic states in central Pb+Pb collisions at  $\sqrt{s_{NN}} = 2.76$  TeV by combining the covariant coalescence model [15] together with a blast-wave-like parametrization [16] for the phase space configurations of constituent particles at freezeout. We demonstrate that while the yields of molecule-state and six-quark-state  $\overline{\Lambda n}$  as well as molecule-state  $\Lambda\Lambda$  are much higher than the experimental upper-limits, the six-quark-state yield of  $\Lambda\Lambda$  could be lower than the experimental upper-limits. Therefore, our results suggest that the current experimental measurement at LHC cannot exclude the existence of the  $\Lambda\Lambda$  as an exotic six-quark state although the  $\Lambda\Lambda$  is unlikely to be a molecular state.

## II. COVARIANT COALESCENCE MODEL

The coalescence model [15, 17–21] and the thermal model [5, 22–26] provide two main approaches to describe the composite particle production in relativistic heavy-ion collisions. The main feature of the coalescence model [17–19] is that the coalescence probability depends on the details of the phase space configurations of the constituent particles at freezeout as well as the statistical weight and wave function of the coalesced cluster, while these details are of no relevance in the thermal model [22–24] of cluster creation. For particle production at mid-rapidity in central Pb+Pb collisions at  $\sqrt{s_{NN}} = 2.76$  TeV considered here, we assume a longitudinal boost-invariant expansion for the constituent particles and the Lorentz invariant one-particle momentum distribution is then given by

$$E \frac{d^3 N}{d^3 p} = \frac{d^3 N}{p_T dp_T d\phi_p dy} = \int d^4 x S(x, p), \quad (1)$$

where  $S(x, p)$  is the emission function which is taken to be a blast-wave-like parametrization as [16]

$$S(x, p) d^4 x = m_T \cosh(\eta - y) f(x, p) J(\tau) d\tau d\eta dr d\phi_s, \quad (2)$$

where  $m_T = \sqrt{m^2 + p_T^2}$  is the transverse mass of the emitted particle and  $f(x, p)$  is the statistical distribution function which is given by  $f(x, p) = g(2\pi)^{-3} [\exp(p^\mu u_\mu / kT) / \xi \pm 1]^{-1}$  with  $g$  being spin degeneracy factor,  $\xi$  the fugacity,  $u_\mu$  the four-velocity of a fluid element in the fireball, and  $T$  the local temperature. The freezeout time is assumed to follow a Gaussian distribution  $J(\tau) = \frac{1}{\Delta\tau\sqrt{2\pi}} \exp(-\frac{(\tau-\tau_0)^2}{2(\Delta\tau)^2})$  with a mean value  $\tau_0$  and a dispersion  $\Delta\tau$ . The transverse rapidity distribution of the fluid element in the fireball is parametrized as  $\rho = \rho_0 r / R_0$  with  $\rho_0$  being the maximum transverse rapidity and  $R_0$  the transverse radius of the fireball [16]. The detailed information can be found in Ref. [27]. In the present coalescence model, the phase space freezeout configuration of constituent particles are thus determined by six parameters, i.e.,  $T$ ,  $\rho_0$ ,  $R_0$ ,  $\tau_0$ ,  $\Delta\tau$  and  $\xi$ .

TABLE I: Parameters of the blast-wave-like analytical parametrization for (anti-)nucleon [27], (anti-)  $\Lambda$  [31] and light quark phase-space configurations for Pb+Pb collisions at  $\sqrt{s_{NN}} = 2.76$  TeV.

|                   | T(MeV) | $\rho_0$ | $R_0$ (fm) | $\tau_0$ (fm/c) | $\Delta\tau$ | $\xi_H$ |         |
|-------------------|--------|----------|------------|-----------------|--------------|---------|---------|
| FOPb-N            | 121.1  | 1.215    | 19.7       | 15.5            | 1.0          | 3.72    |         |
| FOPb- $\Lambda^*$ | 123.4  | 1.171    | 16.7       | 13.1            | 1.0          | 13.64   |         |
|                   | T(MeV) | $\rho_0$ | $R_0$ (fm) | $\tau_0$ (fm/c) | $\Delta\tau$ | $\xi_u$ | $\xi_s$ |
| FOPb-Q            | 154    | 1.08     | 13.6       | 11.0            | 1.3          | 1.02    | 0.89    |

In the coalescence model, the cluster production probability can be calculated through the overlap of the cluster Wigner function with the constituent particle phase-space distribution at freezeout. The invariant momentum distribution of the formed cluster consisting of  $M$  constituent particles can be obtained as

$$E \frac{d^3 N_c}{d^3 P} = E g_c \int \left( \prod_{i=1}^M \frac{d^3 p_i}{E_i} d^4 x_i S(x_i, p_i) \right) \times \rho_c^W(x_1, \dots, x_M; p_1, \dots, p_M) \delta^3(\mathbf{P} - \sum_{i=1}^M \mathbf{p}_i) \quad (3)$$

where  $N_c$  is the multiplicity of the cluster with energy (momentum)  $E$  ( $\mathbf{P}$ ),  $g_c$  is the coalescence factor,  $\rho_c^W$  is the cluster Wigner function and the  $\delta$ -function is adopted to ensure momentum conservation. In this work, the harmonic oscillator wave functions are assumed for the clusters in the rest framework and the corresponding Wigner function is  $\rho_c^W(x_1, \dots, x_M; p_1, \dots, p_M) = \rho^W(q_1, \dots, q_{M-1}, k_1, \dots, k_{M-1}) = 8^{M-1} \exp[-\sum_{i=1}^{M-1} (q_i^2 / \sigma_i^2 + \sigma_i^2 k_i^2)]$ , where  $\mu_{i-1} = \frac{i}{i-1} \frac{m_i \sum_{k=1}^{i-1} m_k}{\sum_{k=1}^{i-1} m_k}$ , ( $i \geq 2$ ) is the reduced mass,  $\sigma_i^2 = (\mu_i w)^{-1}$  ( $1 \leq i \leq M-1$ ), and  $w$  is the harmonic oscillator frequency. The details about the coordinate transformation from  $(x_1, \dots, x_M)[(p_1, \dots, p_M)]$  to relative coordinates  $(q_1, \dots, q_{M-1})[(k_1, \dots, k_{M-1})]$  can be found in Ref. [27]. The mean-square radius is given by  $\langle r_M^2 \rangle = \frac{3}{2Mw} [\sum_{i=1}^M \frac{1}{m_i} - \frac{M}{\sum_{i=1}^M m_i}]$ . The integral (3) can be calculated directly through multi-dimensional numerical integration by Monte-Carlo method [27, 28]. Since the constituent particles may have different freezeout time, in the numerical calculations, the particles that freeze out earlier are allowed to propagate freely until the time when the last particle in the cluster freezes out in order to make the coalescence at equal time [27, 29, 30].

## III. RESULT AND DISCUSSION

### A. Hadron Coalescence

Firstly, we consider  $\Lambda\Lambda$  and  $\overline{\Lambda n}$  as molecular states and their productions in central Pb+Pb collisions at  $\sqrt{s_{NN}} = 2.76$  TeV at LHC can be described by  $\Lambda$ - $\Lambda$

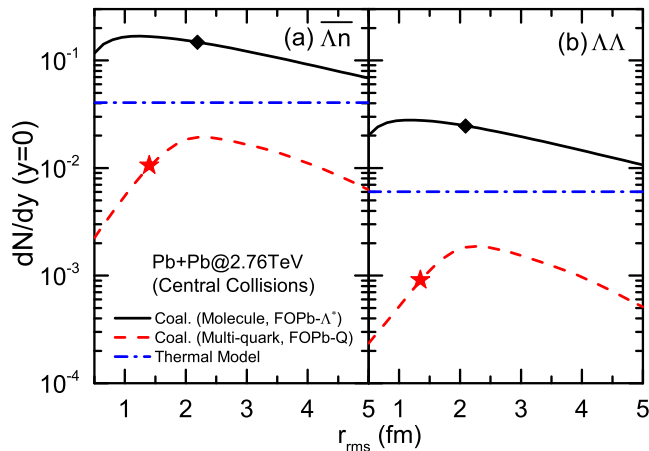


FIG. 1: The yields of  $\overline{\Lambda n}$  (a) and  $\Lambda\Lambda$  (b) versus root-mean-square radii through hadron coalescence and quark coalescence. The diamonds indicate the yield with binding energy  $E_{\text{bind}} = 1$  MeV in the hadron coalescence while the stars represent the yield with a radius obtained from the harmonic oscillator frequency  $w_s$  (see text for the details) in the quark coalescence. The dash-dotted lines are predictions from the thermal model [9].

and  $\overline{\Lambda}\overline{n}$  coalescence, respectively, in the covariant coalescence model. The basic inputs in the present coalescence model calculations are the freezeout configurations of nucleons and  $\Lambda$  particles which can be extracted from experimental information on the production of protons,  $\Lambda$ , light nuclei and light hypernuclei. For central Pb+Pb collisions at  $\sqrt{s_{NN}} = 2.76$  TeV, the freezeout configurations of nucleons (denoted as FOPb-N) and  $\Lambda$  (denoted as FOPb- $\Lambda^*$ ) have been obtained by fitting the experimental spectra of protons,  $\Lambda$ , deuterons and  ${}^3\text{He}$  as well as the measured  ${}^3\text{H}/{}^3\text{He}$  ratio, and the details can be found in Refs. [27, 31]. The parameter values of FOPb-N and FOPb- $\Lambda^*$  are summarized in Table I, and one can see that the protons and  $\Lambda$  have different freezeout configurations with the latter having an earlier mean freezeout time and a smaller freezeout radius to reproduce the measured  ${}^3\text{H}/{}^3\text{He}$  ratio and the  ${}^3\text{H}$  spectrum, as discussed in detail in Ref. [31]. In central Pb+Pb collisions at  $\sqrt{s_{NN}} = 2.76$  TeV, we assume the particles and their anti-partners (as well as protons and neutrons) have the same freezeout configuration.

In the coalescence model, the cluster yield also depends on the cluster size. The root-mean-square radii ( $r_{\text{rms}}$ ) of  $\Lambda\Lambda$  and  $\overline{\Lambda n}$  can be related to their binding energies [13, 14] and their values are treated as free parameters in this work. Fig. 1 shows the  $p_T$ -integrated yield in the mid-rapidity region ( $-0.5 \leq y \leq 0.5$ ) (i.e.,  $dN/dy$  at  $y = 0$ ) of  $\overline{\Lambda n}$  (panel (a)) and  $\Lambda\Lambda$  (panel (b)) versus  $r_{\text{rms}}$  in the range of  $0.5 \sim 5$  fm through hadron coalescence (solid lines). It should be noted that the measured  $\Lambda$  spectrum [32] includes the contributions from strong and electro-magnetic decays but excludes the contributions from weak decays. Following Ref. [14], we as-

sume the measured  $\Lambda$  multiplicity  $N_{\Lambda(1115)}^{\text{measured}} = N_{\Lambda(1115)} + \frac{1}{3}N_{\Sigma(1192)} + (0.87 + \frac{0.11}{3})N_{\Sigma(1385)} = 7.44N_{\Lambda(1115)}$  from which one can easily obtain that the electro-magnetic decay contributes about 16.4% of the total yields. Because the  $\Lambda$  particles coming from electro-magnetic decay of  $\Sigma(1192)$  do not appear in the fireball, thus they should not contribute to the coalescence process and this has been corrected for the results in Fig. 1 and the following analyses. For FOPb-N and FOPb- $\Lambda^*$ , the yield ( $dN/dy$  at  $y = 0$ ) of  $\overline{\Lambda n}$  ranges from  $6.66 \times 10^{-2}$  to  $16.8 \times 10^{-2}$  and the yield of  $\Lambda\Lambda$  ranges from  $1.03 \times 10^{-2}$  to  $2.80 \times 10^{-2}$ . In experimental analysis [9], the binding energy  $E_{\text{bind}}$  of both  $\overline{\Lambda n}$  and  $\Lambda\Lambda$  is assumed to be 1 MeV, and the corresponding  $r_{\text{rms}}$  of  $\overline{\Lambda n}$  and  $\Lambda\Lambda$  are 2.2 fm and 2.1 fm [14], respectively, which are shown by diamonds in the solid lines in Fig. 1. The corresponding yields at  $E_{\text{bind}} = 1$  MeV are  $14.79 \times 10^{-2}$  for  $\overline{\Lambda n}$  and  $2.51 \times 10^{-2}$  for  $\Lambda\Lambda$ . The predictions of a thermal model with a temperature of 156 MeV [9] are also included in Fig. 1 (dash-dotted lines) for comparison. From Fig. 1, one can see that the yields of both  $\overline{\Lambda n}$  and  $\Lambda\Lambda$  from the thermal model can be a few times smaller than that of hadron coalescence, depending on the size of  $\overline{\Lambda n}$  and  $\Lambda\Lambda$ . This feature could be due to the earlier  $\Lambda$  freezeout in the coalescence model, which significantly enhance the yield of light hypernuclei [31].

## B. Quark Coalescence

Now we assume  $\Lambda\Lambda$  and  $\overline{\Lambda n}$  are six-quark states, i.e.,  $\Lambda\Lambda$  is a bound state of  $uuddss$  while  $\overline{\Lambda n}$  is a bound state of  $\overline{u}\overline{d}\overline{d}\overline{u}\overline{s}\overline{s}$ , and their yields can then be calculated through the quark coalescence model. The quark coalescence calculation needs the information of phase-space distributions of  $u, d, s$  quarks and their anti-partners at freezeout, which are determined in the present work by fitting the measured spectra of  $p(uud)$ ,  $\Lambda(uds)$ ,  $\Xi^-(dds)$ ,  $\Omega^-(sss)$  and  $\phi(s\overline{s})$  in the quark coalescence model. In the following, we assume  $u$  and  $d$  quarks have the same mass of 300 MeV while  $s$ -quark mass is 500 MeV. For protons, the mean-square charged radius is found to be  $\langle r_p^2 \rangle = 0.70706 \pm 0.00066$  fm<sup>2</sup> from the recent measurement of muon-atom ( $\mu p$ ) Lamb shift [33], which leads to a harmonic oscillator frequency ( $w$ ) of 0.184 GeV for the proton wave function. For  $\Lambda$ ,  $\Xi^-$ ,  $\Omega^-$  and  $\phi$ , their radii are unknown and generally depend on model predictions. For simplicity, following Refs. [13, 14], we assume the harmonic oscillator wave functions of these strange hadrons share the same frequency  $w_s$ . For  $\Omega^-$ , LQCD simulation found  $\sqrt{\langle r_{\Omega^-}^2 \rangle} = 0.573 - 0.596$  fm [34], while a recent work based on a combined chiral and  $1/N_C$  expansions method found that  $\sqrt{\langle r_{\Omega^-}^2 \rangle} = 1.0$  fm [35] gives a better  $\chi^2$  fit for mean-square charge radii of baryons. We have tried both values, and find that  $\sqrt{\langle r_{\Omega^-}^2 \rangle} = 1.0$  fm gives a better fit of the measured spectra of these

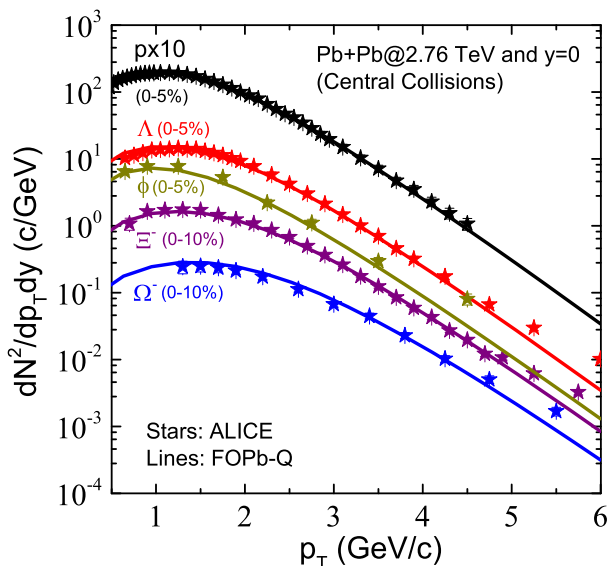


FIG. 2: Transverse momentum distributions of hadrons in central Pb+Pb collisions at  $\sqrt{s_{NN}} = 2.76$  TeV. The experimental results (stars) are taken from ALICE measurement [32, 36–38]. The solid lines are from the quark coalescence model. The results of protons have been multiplied by a factor of 10.

strange hadrons and thus the corresponding frequency  $w_s$  is 0.078 GeV. Table II summarizes the corresponding root-mean-square radii of hadrons and the coalescence factors  $g_c$  including spin and color degree of freedom.

TABLE II: The root-mean-square radii of hadrons and corresponding coalescence factor  $g_c$ , including the spin and color degree of freedom.

| Hadron                | $p$                        | $\phi$                     | $\Xi$                      | $\Omega$                   | $\Lambda$                  |
|-----------------------|----------------------------|----------------------------|----------------------------|----------------------------|----------------------------|
| $r_{\text{rms}}$ (fm) | 0.84                       | 0.87                       | 1.1                        | 1.0                        | 1.2                        |
| $g_c$                 | $\frac{2}{3^3 \times 2^3}$ | $\frac{3}{3^2 \times 2^2}$ | $\frac{2}{3^3 \times 2^3}$ | $\frac{4}{3^3 \times 2^3}$ | $\frac{2}{3^3 \times 2^3}$ |

The weak decay contributions from heavier hadrons have been already excluded in the experimental spectra of  $p$ ,  $\Lambda$ ,  $\Xi^-$ ,  $\Omega^-$  and  $\phi$ , but not for the strong and electro-magnetic decays. In order to compare with experimental data, we have to include these effects in quark coalescence calculations. Following Refs. [13, 14], we assume the relations  $N_{\Lambda(1115)}^{\text{measured}} = N_{\Lambda(1115)} + \frac{1}{3}N_{\Sigma(1192)} + (0.87 + \frac{0.11}{3})N_{\Sigma(1385)} = 7.44N_{\Lambda(1115)}$ ,  $N_p^{\text{measured}} = N_p + N_{\Delta^{++}(1232)} + \frac{1}{2}N_{\Delta^+(1232)} + \frac{1}{2}N_{\Delta^0(1232)} = 5N_p$ , and  $N_{\Xi^-}^{\text{measured}} = N_{\Xi^-} + \frac{1}{2}N_{\Xi(1530)} = 3N_{\Xi^-}$ . For  $\phi$  and  $\Omega^-$ , we assume no strong and electro-magnetic decay corrections, and thus  $N_{\phi}^{\text{measured}} = N_{\phi}$ ,  $N_{\Omega^-}^{\text{measured}} = N_{\Omega^-}$ . In the above,  $N_{\Lambda(1115)}$ ,  $N_p$ ,  $N_{\Xi^-}$ ,  $N_{\phi}$  and  $N_{\Omega^-}$  represent the corresponding hadron multiplicity obtained directly from the quark coalescence model.

By fitting simultaneously the measured transverse momentum spectra of  $p$  [36],  $\Lambda$  [32],  $\phi$  [37],  $\Xi^-$  [38], and

$\Omega^-$  [38] for central Pb+Pb collisions at  $\sqrt{s_{NN}} = 2.76$  TeV, the parameters of the phase-space freezeout configuration are extracted and summarized as FOPb-Q in Table I. The temperature is fixed as  $T = 154$  MeV [39, 40], and the extracted transverse flow rapidity parameter is  $\rho_0 = 1.08$ , the transverse radius is  $R_0 = 13.6$  fm, the mean longitudinal proper freezeout time is  $\tau_0 = 11.0$  fm/c, the proper time dispersion is  $\Delta\tau = 1.3$  fm/c, and the fugacity is 1.02 for  $u$  and  $d$  quarks and 0.89 for  $s$ -quarks. Fig. 2 compares the theoretical calculations with the experimental data for the hadron transverse momentum spectra. In the theoretical calculations, as mentioned earlier, the contributions from the strong and electro-magnetic decays have been included to compare with the measured data. One can see that the fit is very nice, and the obtained quark freezeout configuration FOPb-Q can thus be used to predict the corresponding yields of  $\Lambda\Lambda$  and  $\bar{\Lambda}\bar{n}$  through the quark coalescence model.

The dashed lines in Fig. 1 represent the  $r_{\text{rms}}$  dependence of the yields of six-quark-state  $\bar{\Lambda}\bar{n}$  and  $\Lambda\Lambda$  through quark coalescence using FOPb-Q. The yield of  $\bar{\Lambda}\bar{n}$  ranges from  $22.4 \times 10^{-4}$  to  $20.0 \times 10^{-3}$  and correspondingly the yield of  $\Lambda\Lambda$  ranges from  $2.35 \times 10^{-4}$  to  $1.95 \times 10^{-3}$ . If we assume the harmonic oscillator frequencies for  $\bar{\Lambda}\bar{n}$  and  $\Lambda\Lambda$  are the same as  $w_s$ , their  $r_{\text{rms}}$  are then found to be 1.4 fm and 1.35 fm, respectively, which are indicated by stars in Fig. 1 and the corresponding yields are  $10.6 \times 10^{-3}$  and  $9.11 \times 10^{-4}$ , respectively. It is seen that the predicted yields by the quark coalescence are much smaller than that of the hadron coalescence. This difference is mainly due to the fact that in the hadron coalescence, the strong decays dominantly contribute to the nucleon and  $\Lambda$  multiplicities, which will significantly enhance the yields of  $\bar{\Lambda}\bar{n}$  and  $\Lambda\Lambda$  through  $\bar{\Lambda}\bar{n}$  and  $\Lambda\Lambda$  coalescence, respectively. In the quark coalescence, on the other hand, the six-quark-state  $\bar{\Lambda}\bar{n}$  and  $\Lambda\Lambda$  can only be produced directly from the quark coalescence.

### C. Comparison with experimental limits

Experimentally, no signals of bound states of  $\bar{\Lambda}\bar{n}$  and  $\Lambda\Lambda$  are observed in central Pb+Pb collisions at  $\sqrt{s_{NN}} = 2.76$  TeV, and instead the upper-limits of these particle yields are obtained [9]. Shown in Fig. 3 is the comparison of the yields ( $dN/dy$  at  $y = 0$ ) of  $\bar{\Lambda}\bar{n}$  (panel (a)) and  $\Lambda\Lambda$  (panel (b)) verse decay length (lifetime) between experimental upper-limits and theoretical calculations, and here a preferred branching ratio of 64% [41] is used for  $\Lambda\Lambda \rightarrow \Lambda p \pi^-$  and 54% [42] for  $\bar{\Lambda}\bar{n} \rightarrow d \pi^+$ . It is very interesting to see that while the predicted yield of  $\bar{\Lambda}\bar{n}$  in either molecular state or six-quark state is higher than the experimental upper-limit, the yield of six-quark-state  $\Lambda\Lambda$  could be lower than the experimental upper-limit although the yield of molecule-state  $\Lambda\Lambda$  is higher than the upper-limit. These features indicate that the bound state of  $\bar{\Lambda}\bar{n}$  is unlikely to exist, either in molecular or in

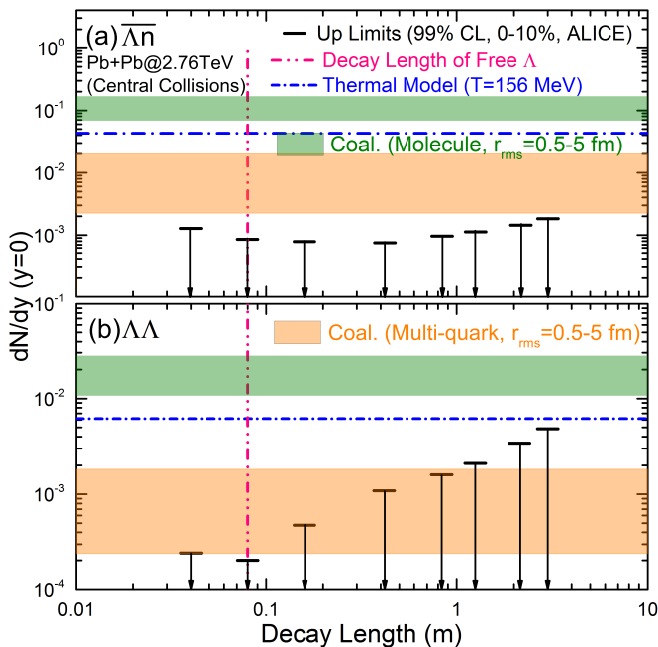


FIG. 3: Comparison between experimental upper-limits and theoretical calculations for the yields of  $\bar{\Lambda}n$  (a) and  $\Lambda\Lambda$  (b). A preferred branching ratio of 64% [41] is used for  $\Lambda\Lambda \rightarrow \Lambda p\pi^-$  and 54% [42] for  $\bar{\Lambda}n \rightarrow \bar{d}\pi^+$ . The experimental results are taken from ALICE measurement [9]. The olive shaded regions and the orange bands are predictions of molecular states and multi-quark states from hadron coalescence and quark coalescence, respectively.

six-quark state, which is consistent with the conclusion obtained from experimental analyses by the HypHI Collaboration [43]. Meanwhile, the molecular state of  $\Lambda\Lambda$  is unlikely to exist either. However, the six-quark state of  $\Lambda\Lambda$  could exist, and cannot be excluded by the ALICE measurement.

In Fig. 3, the branching ratios of  $\Lambda\Lambda \rightarrow \Lambda p\pi^-$  and  $\bar{\Lambda}n \rightarrow \bar{d}\pi^+$  are fixed at their preferred values which are obtained in model prediction. To see the branching ratio dependence of our conclusion, we present in Fig. 4 the comparison for the yields between experimental upper-limits of  $\bar{\Lambda}n$  (panel (a)) and  $\Lambda\Lambda$  (panel (b)) with a lifetime of free  $\Lambda$  and the corresponding theoretical calculations for different decay branching ratios. The dashed lines show the predictions from hadron coalescence with a binding energy  $E_b = 1$  MeV and the bands correspond to the results from quark coalescence with radius from 0.5 fm to 5 fm. One can see the yields of molecular states are much higher than the upper-limits in almost the whole range of decay branching ratio. The yield of six-quark-state  $\bar{\Lambda}n$  can be consistent with experimental upper-limits only when the decay branching ratio is smaller than 0.2 which is much smaller than the preferred value, while the yield of six-quark-state  $\Lambda\Lambda$  is consistent with experimental upper-limits even assuming the decay branching ratio is as large as 0.7 which is larger than the preferred value.

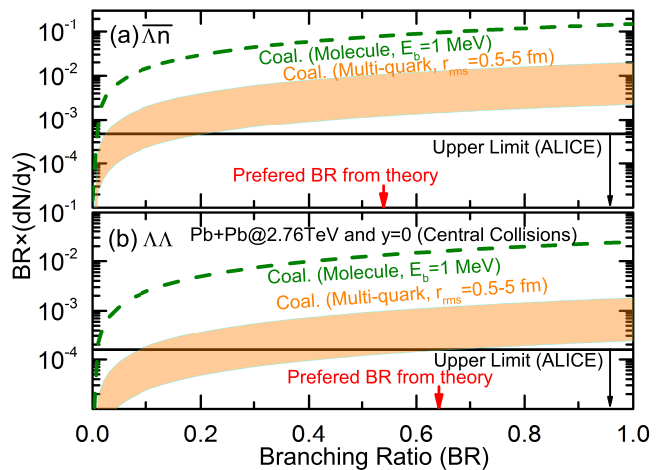


FIG. 4: Comparison between experiment upper-limits under the assumption of the lifetime of a free  $\Lambda$  and theoretical calculations for the yields of  $\bar{\Lambda}n$  (a) and  $\Lambda\Lambda$  (b). The dashed lines represent the molecular states from hadron coalescence with a binding energy  $E_{\text{bind}} = 1$  MeV and the bands correspond to multi-quark states from quark coalescence with  $r_{\text{rms}} = 0.5 \sim 5$  fm.

#### IV. CONCLUSION

Based on a covariant coalescence model with a blast-wave-like analytical parametrization for the phase-space configuration of the constituent particles, we have elaborately studied the productions of  $\bar{\Lambda}n$  and  $\Lambda\Lambda$  in central Pb+Pb collisions at  $\sqrt{s_{NN}} = 2.76$  TeV. Their yields are calculated either through hadron coalescence or quark coalescence. In the hadron coalescence, the two states are considered as molecular states, and the freezeout phase-space configurations of nucleons and  $\Lambda$  are extracted through fitting the measured spectra of light nuclei and hypernuclei. In the quark coalescence, the two states are considered as six-quark states, and the freezeout phase-space configuration of light and strange quarks are extracted through fitting the measured spectra of  $p$ ,  $\Lambda$ ,  $\phi$ ,  $\Xi^-$ , and  $\Omega^-$ .

Our results have indicated that the yields of  $\bar{\Lambda}n$  and  $\Lambda\Lambda$  in multi-quark states from quark coalescence are much lower than that in molecular states from hadron coalescence. This is mainly due to the dominant strong decay contributions into nucleons and  $\Lambda$  which can significantly enhance the molecule-state yields through hadron coalescence. In particular, we have found that although the predicted yields of molecule-state  $\bar{\Lambda}n$  and  $\Lambda\Lambda$  as well as six-quark-state  $\bar{\Lambda}n$  are higher than the experimental upper-limits, the yield of six-quark-state  $\Lambda\Lambda$  could be lower than the upper-limits. Therefore, the molecular or six-quark  $\bar{\Lambda}n$  as well as molecular  $\Lambda\Lambda$  are unlikely to be bound states. However, the six-quark-state  $\Lambda\Lambda$  could be a bound state and cannot be excluded by the ALICE measurement. If  $\Lambda\Lambda$  is a multi-quark state, then according to the predicted yield in the present work, we are

likely at the edge of discovering it.

### Acknowledgments

We are grateful to Jia-Lun Ping, Rui-Qin Wang and Zhong-Bao Yin for helpful discussions. This work was supported in part by the Major State Basic Research Development Program (973 Program) in China under Con-

tract Nos. 2015CB856904 and 2013CB834405, the NSFC under Grant Nos. 11625521, 11275125 and 11135011, the “Shu Guang” project supported by Shanghai Municipal Education Commission and Shanghai Education Development Foundation, the Program for Professor of Special Appointment (Eastern Scholar) at Shanghai Institutions of Higher Learning, and the Science and Technology Commission of Shanghai Municipality (11DZ2260700).

- 
- [1] R. L. Jaffe, *Phys. Rev. Lett.* **38**, 195 (1977).  
 [2] S. R. Beane et al., *Phys. Rev. Lett.* **106**, 162001 (2011).  
 [3] T. Inoue et al., *Phys. Rev. Lett.* **106**, 162002 (2011).  
 [4] T. Doi et al. [HAL QCD Collaboration], arXiv:1512.01610; arXiv:1512.04199.  
 [5] J. Steinheimer et al., *Phys. Lett.* **B714**, 85 (2012).  
 [6] L. Adamczyk et al. [STAR Collaboration], *Phys. Rev. Lett.* **114**, 022301 (2015).  
 [7] K. Morita, T. Furumoto, and A. Ohnishi, *Phys. Rev. C* **91**, 024916 (2015).  
 [8] A. Ohnishi, K. Morita, K. Miyahara, and T. Hyodo, arXiv:1603.05761.  
 [9] J. Adam et al. [ALICE Collaboration], *Phys. Lett.* **B752**, 267 (2016).  
 [10] J. Stachel, A. Andronic, P. Braun-Munzinger, and K. Redlich, *J. Phys.: Conf. Series* **509**, 012019 (2014).  
 [11] G. Torrieri, S. Steinke, W. Broniowski, W. Florkowski, J. Letessier, and J. Rafelski, *Comput. Phys. Commun.* **167**, 229 (2005).  
 [12] G. Torrieri, S. Jeon, J. Letessier, and J. Rafelski, *Comput. Phys. Commun.* **175**, 635 (2006).  
 [13] S. Cho et al., *Phys. Rev. Lett.* **106**, 212001 (2011).  
 [14] S. Cho et al., *Phys. Rev. C* **84**, 064910 (2011).  
 [15] C. B. Dover, U. Heinz, E. Schnedermann, and J. Zimanyi, *Phys. Rev. C* **44**, 1636 (1991).  
 [16] F. Retière and M. A. Lisa, *Phys. Rev. C* **70**, 044907 (2004).  
 [17] S. T. Butler and C. A. Pearson, *Phys. Rev. Lett.* **7**, 69 (1961).  
 [18] H. Sato and K. Yazaki, *Phys. Lett.* **B98**, 153 (1981).  
 [19] L. P. Csernai and J. I. Kapusta, *Phys. Rep.* **131**, 223 (1986).  
 [20] Y. Oh, Z. W. Lin, and C. M. Ko, *Phys. Rev. C* **80**, 064902 (2009).  
 [21] L. Xue, Y. G. Ma, J. H. Chen, and S. Zhang, *Phys. Rev. C* **85**, 064912 (2012); *Phys. Rev. C* **92**, 059901 (2015).  
 [22] J. Cleymans et al., *Z. Phys. C* **51**, 137 (1991).  
 [23] P. Braun-Munzinger and J. Stachel, *J. Phys. G* **21**, L17 (1995); *Nature* **448**, 302 (2007).  
 [24] J. Cleymans and K. Redlich, *Phys. Rev. C* **60**, 054908 (1999).  
 [25] A. Andronic, P. Braun-Munzinger, J. Stachel, and H. Stöcker, *Phys. Lett.* **B697**, 203 (2011).  
 [26] J. Cleymans et al., *Phys. Rev. C* **84**, 054916 (2011).  
 [27] K. J. Sun and L. W. Chen, *Phys. Lett.* **B751**, 272 (2015).  
 [28] G. P. Lepage, *J. Comput. Phys.* **27**, 192 (1978).  
 [29] R. Mattiello, H. Sorge, H. Stöcker, and W. Greiner, *Phys. Rev. C* **55**, 1443 (1997).  
 [30] L. W. Chen and C. M. Ko, *Phys. Rev. C* **73**, 044903 (2006).  
 [31] K. J. Sun and L. W. Chen, *Phys. Rev. C* **93**, 064909 (2016) [arXiv:1512.00692].  
 [32] B. Abelev et al. [ALICE Collaboration], *Phys. Rev. Lett.* **111**, 222301 (2013).  
 [33] K. A. Olive et al. [Particle Data Group Collaboration], *Chin. Phys. C* **38**, 090001 (2014).  
 [34] C. Alexandrou et al., *Phys. Rev. D* **82**, 034504 (2010).  
 [35] R. Flores-Mendieta and M. A. Rivera-Ruiz, *Phys. Rev. D* **92**, 094026 (2015).  
 [36] B. Abelev et al. [ALICE Collaboration], *Phys. Rev. Lett.* **109**, 252301 (2012).  
 [37] B. Abelev et al. [ALICE Collaboration], *Phys. Rev. C* **91**, 024609 (2015).  
 [38] B. Abelev et al. [ALICE Collaboration], *Phys. Lett.* **B728**, 216 (2014).  
 [39] A. Bazavov et al, *Phys. Rev. D* **85**, 054503 (2012).  
 [40] A. Bazavov et al, *Phys. Rev. D* **90**, 094503 (2014).  
 [41] J. Schaffner-Bielich, R. Mattiello, and H. Sorge, *Phys. Rev. Lett.* **84**, 4305 (2000).  
 [42] J. Schaffner-Bielich, calculations based on [41], 2012.  
 [43] C. Rappold et al. [HypHI Collaboration], *Phys. Rev. C* **88**, 041001(R) (2013).